# Unusual angular momentum transfer in electron-impact excitation of neon

L. R. Hargreaves, C. Campbell, M. A. Khakoo, Oleg Zatsarinny, and Klaus Bartschat

Phys. Rev. A **85**, 050701 — Published 22 May 2012

DOI: 10.1103/PhysRevA.85.050701

# Unusual Angular Momentum Transfer in Electron-Impact Excitation of Neon

L. R. Hargreaves, C. Campbell, M. A. Khakoo
*Department of Physics, California State Fullerton, Fullerton, CA 92831, USA*

Oleg Zatsarinny, Klaus Bartschat
*Department of Physics and Astronomy, Drake University, Des Moines, IA 50311, USA*

(Dated: April 13, 2012)

We report results from a joint experimental/theoretical study of the angular momentum transfer in electron impact excitation of the $(2p^6)^1S_0 \rightarrow (2p^5 3s)^1P_1$ resonance transition in Ne. Both the measured and calculated data show the circular light polarization $P_3$ to be positive for an incident energy of 25 eV at scattering angles below 40°. This observation implies a negative angular momentum transfer $L_\perp$, which is the opposite sign of orientation expected from a well-known propensity rule for $S \rightarrow P$ excitation at small scattering angles.

PACS numbers: 34.80.Bm,34.80.Dp

Extensive work on the orientation of atoms excited by electron impact strongly supports an empirical "propensity rule", indicating that the sign of the angular momentum transfer, $L_\perp^+$, is positive for $S \rightarrow P$ transitions at small scattering angles, essentially independent of the projectile energy or the specific target [1]. Interest in the generality of this rule, and any physical basis for it, stems from the early work of Kohmoto and Fano [2], who considered a classical grazing-incidence collision from the attractive potential between the projectile electron and the target, which results in the excited state having a positive orbital angular momentum component perpendicular to the scattering plane. Further work on this problem was performed by Madison and Winters [3], who pointed out a phase error in [2] and then analyzed the orientation in terms of the projectile charge in a perturbation series expansion. They predicted a difference in the sign of $L_\perp^+$ between electron and positron impact at small scattering angles, but without being able to predict the actual sign for either case.

Andersen and Hertel [4] later developed a semiclassical model. While its validity was limited to small scattering angles, the model did offer the general prediction that the angular momentum transfer for electron impact excitation processes was positive. Attempts to check the predictions of this model were made in a pioneering experiment reported by Shurgalin *et al.* [5] who studied electron scattering from the laser-excited $3p$ state in Na. Comparing deexcitation to the $3s$ ground state in superelastic collisions with excitation to the $4s$ state in inelastic collisions, their results ultimately remained inconclusive for the $4s$ state. Bartschat *et al.* [6] explained the findings of Shurgalin *et al.* by noting that the simple Andersen-Hertel model is not applicable to the Na $(4s)$ case, due to the very large dipole polarizability of this state, which leads to an additional attractive potential that was neglected in the semiclassical argument.

Extensive compilations [1] of the available experimental data at the time, and many more theoretical predictions, showed the propensity for a positive angular momentum transfer at small scattering angles in $S \rightarrow P$ excitation to be seemingly very well fulfilled for the case of unpolarized incident electrons. An important generalization was presented by Andersen *et al.* [7], who analyzed the so-called "generalized Stokes parameters" [8, 9] for a spin-polarized projectile beam. They found that parity conservation required the opposite sign of $L_\perp^+$ for spin-up and spin-down (relative to the scattering plane) electrons for forward scattering. Once again, however, they noticed that the spin-averaged value in electron-impact excitation of the $(6s6p)^3P_1$ state in Hg fulfilled the propensity rule very well. This was also confirmed in an extensive compilation of data for spin-resolved electron impact [10].

Here we report both measured and calculated electron impact coherence parameters (EICPs) for excitation of the $(2p^6)^1S_0 \rightarrow (2p^5[1/2]3s)^1P_1$ VUV transition (excitation energy = 16.848 eV) in Ne at a number of collision energies. [Although the excited state is often written in intermediate coupling as a combination of a $^1P_1$ and $^3P_1$ states, we use the more familiar $LS$ notation here, since the dominant character of the state is still $^1P_1$.] At 25 eV incident energy, both experiment and theory show $L_\perp^+$ to be *negative* at scattering angles $0 \leq \theta \leq 40°$, with a minimum near $\theta = 30°$.

The setup of the experiment, shown in Fig. 1, is similar to that given in [11]. The apparatus consists of an electron energy-loss spectrometer coupled with a vacuum-ultraviolet (VUV) polarizer, which is housed in a high-vacuum chamber made from stainless steel. The chamber was evacuated by a 6" turbomolecular pump providing an oil-free vacuum environment. Backing pump oil was inhibited from streaming up the vacuum line into the pump by using a micro-maze oil filter. The base pressure of the vacuum system was $1.5 \times 10^{-7}$ torr. Neon gas was delivered to the collision region via a 50 mm long molybdenum needle, of internal diameter 1 mm, that was driven with a pressure of 0.35 torr. The needle was aligned perpendicular to the electron beam whilst laying in the scattering plane (i.e., not pointing into the photon polarizer). With the gas flowing, the vacuum chamber pressure was $5 \times 10^{-7}$ torr. In this pressure regime, we expect radiation trapping to be negligible [11].

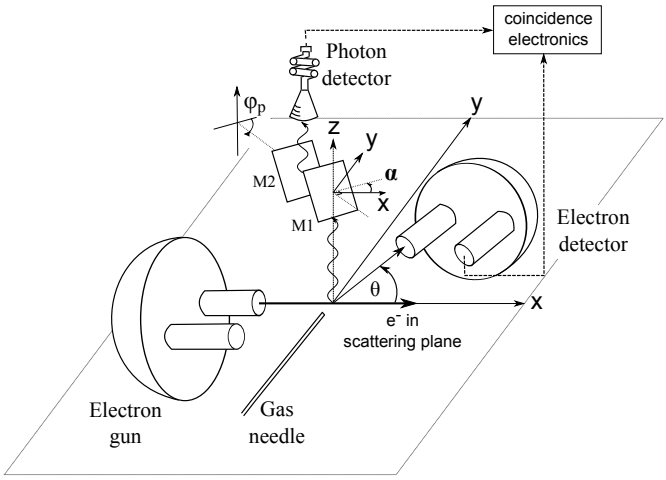


FIG. 1: Sketch of the experimental setup. See text for details. Note that $\phi_p = 0^\circ$ for the arrangement of M1 and M2 shown.

The electron spectrometer, described in a prior publication [12], employed hemispherical energy selectors in the electron gun and analyzer regions. The spectrometer operated with a total energy resolution of 600 meV (FWHM) and produced electron beam currents between 1.0 and 1.5 $\mu$A. This energy resolution was insufficient to resolve the $(2p^5[1/2]3s)^1P_1$ and $(2p^5[3/2]3s)^3P_1$ excited levels. The dominant $^3P_1$ character of the latter, however, leads to a much smaller excitation cross section compared to the $^1P_1$ state at an incident energy of 25 eV. Coupled with its much longer lifetime $^3P_1$ (21.0 ns versus 1.64 ns [13]), the contribution of the $^3P_1$ state to the coincident signal was negligible, especially at small $\theta$.

VUV photons emitted from collision events were detected by a double reflection polarizer mounted perpendicular to the scattering plane. The principles of a reflection optics polarizer are described in detail in [11] and [14]. Briefly, the polarizer consisted of two gold-plated mirrors (M1 and M2 in Fig. 1) that were flat to 1/10 of a wavelength (for $\lambda = 632$ nm [15]) and whose normal vectors were mounted at reflection angles of 57.6° to the incident light. Linearly polarized light was measured by physically rotating M1 and M2 around the photon emission axis (angle $\alpha$ in Fig. 1), while holding M1 and M2 parallel to each other ($\phi_p = 0^\circ$ in Fig. 1). To measure the circular polarization the polarizer was aligned at $\alpha = \pm 45^\circ$ to the major axis of the emitted radiation's polarization ellipse while M2 was rotated to $\phi_p \pm 45^\circ$ to behave as a quarter-wave plate.

The techniques used for determining the polarization efficiencies of the VUV polarizer were similar to those reported in [11] and will be elaborated on in a future publication. We note, however, that all measured data were corrected for the polarizer's linear and circular polarization efficiencies for all VUV transition lines of interest. These efficiencies were determined from the experimental optical refractive index and extinction values of the gold mirrors [16], using the appropriate formulae given in [17]. Test measurements of the EICPs for helium were performed at an incident energy of $E_0 = 50$ eV, for the $(1s^2)^1S \rightarrow (1s2p)^1P$ transition, to ensure the validity of our polarization efficiencies. The results were in very good agreement with the published data [1] and confirmed a positive $L_\perp^+$ at small $\theta$.

Output pulses from the polarizer and electron spectrometer were amplified and passed to a time-to-amplitude converter (Ortec 566) connected to a pulse-height analyzer (Ortec Easy-MCA 2K). Time-coincident electron/photon events were recorded and analyzed by a data acquisition PC (Dell Inspiron 560), which also monitored the experiment and was responsible for setting and changing the position of the polarizer. Custom data acquisition software was developed in-house for this study, using Labview 2010. Data acquisition times per point ranged from two days to over two weeks, depending on the signal levels at each $\theta$.

The theoretical predictions shown below were obtained from an extension of previous work [18] on this problem. Specifically, we used the BSR code [19] to perform a semi-relativistic (Breit-Pauli) $R$-matrix (close-coupling) calculation for e-Ne collisions. The original 31-state model [18] was extended to a total of up to 457 coupled states, in order to account for coupling to the ionization continuum and to represent the polarizabilities of the states involved. This 457-state model is expected to give well-converged results not only in the near-threshold resonance regime, but also at the "intermediate" energies of the present work. In fact, however, convergence tests (see below) showed that models with less coupled states already predict qualitatively similar results.

Figure 2 shows the measured light polarizations

$$P_1 = \frac{I_0 - I_{90}}{I_0 + I_{90}}, \quad (1)$$

$$P_2 = \frac{I_{45} - I_{135}}{I_{45} + I_{135}}, \quad (2)$$

$$P_3 = \frac{I_{\rm rhc} - I_{\rm lhc}}{I_{\rm rhc} + I_{\rm lhc}}, \quad (3)$$

for the photon detector located perpendicular to the scattering plane [9]. Here $I_\alpha$ is the intensity passed through the linear polarizer, with transmission direction oriented at an angle $\alpha$ relative to the incident beam axis, while $I_{\rm rhc}$ ($I_{\rm lhc}$) denotes the intensity of right-hand (left-hand) circularly polarized light.

From the above measurements one can derive the EICPs that describe the charge cloud of the excited state [1, 9]. The degree of linear polarization is

$$P_l = \sqrt{P_1^2 + P_2^2}, \quad (4)$$

and the alignment angle is derived from

$$\tan(2\gamma) = P_2/P_1. \quad (5)$$

As mentioned above, the angular momentum $L_\perp^+$ imparted to the excited state is related to the circular light

polarization through [1]

$$L_{\perp}^{+} = -P_3. \tag{6}$$

Finally, the total degree of polarization is defined as

$$P = \sqrt{P_1^2 + P_2^2 + P_3^2}. \tag{7}$$

For the case at hand, another independent parameter is the height of the charge cloud ($h$), which can be determined from a third linear polarization measurement ($P_4$) with a photon detector located in the collision plane [9]. For the cases shown below, however, $h$ is too small to be distinguished from zero experimentally.

The derived EICPs are shown in Fig. 3. The total degree of polarization is an indicator for the level of coherence in the process. For a fully coherent excitation and detection process, $P \equiv 1$. A reduction in the measured coherence may occur for several reasons, including explicitly spin-dependent forces such as the spin-orbit interaction, either in the target or between the projectile and the target, or depolarization due to the hyperfine interaction. The former can be accounted for through the height of the charge cloud while the latter may be treated through so-called "perturbation coefficients" [9]. However, since the only stable isotope with non-vanishing nuclear spin represents merely 0.27% of the natural isotope mixture in Ne [20], this effect is negligible.

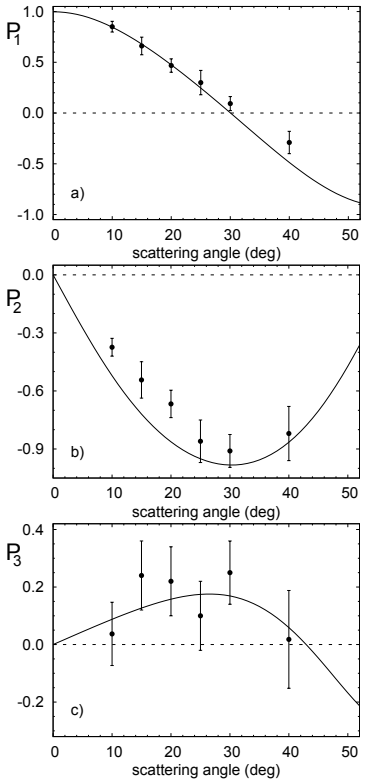


FIG. 2: Light polarizations of the VUV radiation measured in the present experiment after electron impact excitation of the $(2p^6)^1S_0 \rightarrow (2p^5 3s)^1P_1$ resonance transition in Ne at an incident electron energy of 25 eV, in comparison to the BSR predictions.

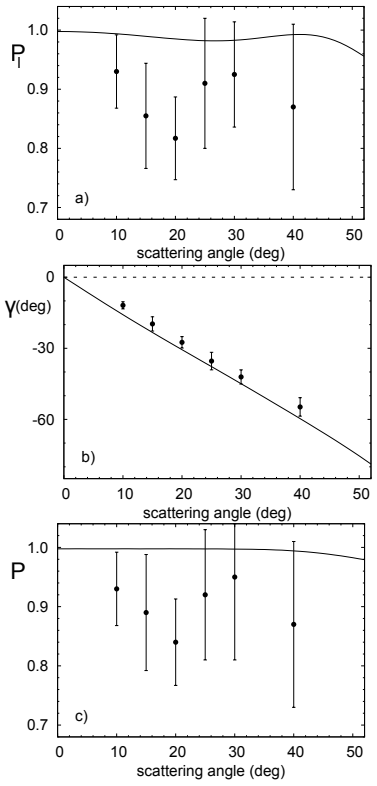


FIG. 3: EICPs derived from the measurements shown in Fig. 2, in comparison to the BSR predictions.

There is very good agreement between the measured and calculated data for both $P_1$ and $P_3$ (top and bottom panels of Fig. 2). The experimental $P_2$ values are slightly smaller in magnitude at small $\theta$ than predicted by the BSR model, although the overall agreement for $P_2$ is still encouraging. The measured values of $P_l$ are also slightly lower than predicted by the BSR calculation at small $\theta$, due to the difference in the $P_2$ data. The agreement for the alignment angle $\gamma$ (center panel of Fig. 3) is excellent. Since this angle is critical for positioning the VUV polarizer to properly measure $P_3$, the level of agreement seen here is highly encouraging.

While the measured values of $P_3 = -L_{\perp}^{+}$ are all small (less than 0.2, which is comparable to the experimental uncertainty), the data are nonetheless clearly positive for all six measured scattering angles between 10° and 40°, three of which are non-zero by two error bars. This result shows a clear exception to the empirical propensity that $L_{\perp}^{+}$ is strictly positive at small scattering angles.

After finding this rather surprising result, we looked for possible explanations. One peculiarity of the heavy noble gases in this particular transition, compared to H, He, the alkalis, and the alkaline-earth elements, all of which seem to fulfill the propensity rule very well, is the fact that the $S \rightarrow P$ transition between states of total orbital angular momentum occurs via a $p \rightarrow s$ transition of the active

electron, i.e., the $P$ state is made by a hole rather than by the active electron gaining both energy and orbital angular momentum. Hence, it seemed conceivable that the effect might occur over a significant energy range, as well as in Ar, Kr, and Xe. Since the simpler distorted-wave approaches did not indicate this behavior [1], we also investigated the level of sophistication necessary in the numerical model to show the effect.

Figures 4, 5, and 6 exhibit samples of our results. From Fig. 4, we see that largest value of $P_3$ occurs for an energy around 25 eV, while the effect is reduced for lower and higher energies. The $^3P_1$ state violates the propensity rule even more, but this prediction would be hard to test experimentally.

Figure 5 presents a convergence test of the close-coupling expansion. The simplest 5-state model, which only couples the ground state and the four states of the $(2p^5 3s)$ manifold, does *not* yield a violation of the propensity rule. This explains why the effect was not seen in distorted-wave models [1]. The 15-state model, however, already shows the effect and gives qualitatively good agreement with our most sophisticated 457-state predictions. For the linear polarization $P_2$, on the other hand, there is almost no dependence of the results on the number of coupled states. The same statement holds for $P_1$, and this explains the lack of sensitivity of $\gamma$ to the details of the model.

Finally, Fig. 6 shows that the effect seen in the present work for Ne for an incident energy around 25 eV is a truly usual case and an exception to the rule. BSR calculations for Ar (31 coupled states), Kr (69 states) and Xe (75 states) all revealed "normal" behavior. We first suspected the importance of interference between the amplitudes for excitation of the singlet and triplet parts of the wavefunction and, consequently, lowered the collision energy for the heavier targets to account for the reduced ionization potential. Extensive tests, however, revealed that the normal behavior is once again independent of the particular energy over a wide range.

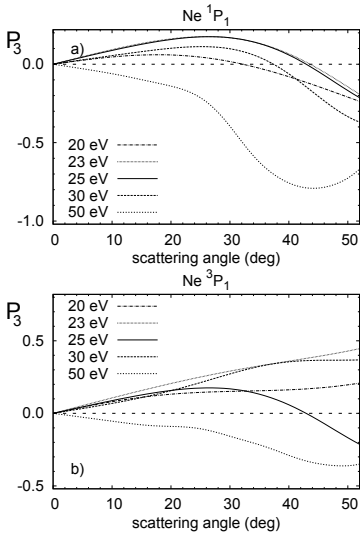


FIG. 4: Circular light polarization $P_3$ for a number of incident energies, as predicted by the BSR-457 model.

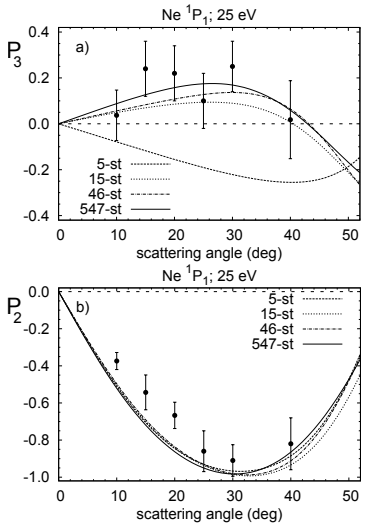


FIG. 5: Circular light polarization $P_3$ and linear polarization $P_2$ the Ne $^1P_1$ state, as predicted by the BSR model with different numbers of coupled states.

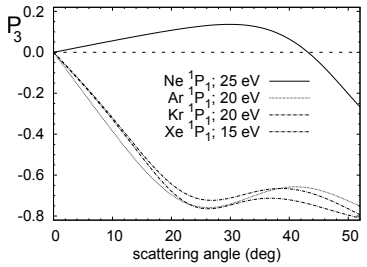


FIG. 6: Circular light polarization $P_3$ for Ne, Ar, Kr, and Xe, as predicted by the BSR model.

In conclusion: We predicted a rare exception to the propensity rule of a positive angular momentum transfer in electron-impact excitation of an $S \rightarrow P$ transition at small scattering angles. The prediction was confirmed by a highly challenging electron-photon coincidence experiment with VUV radiation. The effect is apparently due to complex channel coupling and seems to be peculiar to the Ne target. No simple explanation is currently available, but further studies are planned in the future.

This work was supported by the United States National Science Foundation under grants RUI-PHY-0965793 (LRH, CC, MAK), PHY-0903818 (OZ and KB), and PHY-1068140 (KB). We thank Dr. J. W. McConkey (Univ. of Windsor, Ontario, Canada) for providing the VUV polarizer from his laboratory.

[1] N. Andersen, J. W. Gallagher, and I. V. Hertel, Phys. Rep. **180** (1988) 1.
[2] M. Kohmoto and U. Fano, J. Phys. B **14** (1981) L447.
[3] D. H. Madison and K. H. Winters, Phys. Rev. Lett. **47** (1981) 1885.
[4] N. Andersen and I. V. Hertel, Comments At. Mol. Phys. **19** (1986) 1.
[5] M. Shurgalin, A. J. Murray, W. R. MacGillivray, M. C. Standage, D. H. Madison, K. D. Winkler, and I. Bray, Phys. Rev. Lett. **81** (1998) 4604.
[6] K. Bartschat, N. Andersen, and D. Loveall, Phys. Rev. Lett. **83** (1999) 5254.
[7] N. Andersen, K. Bartschat, G.F. Hanne, and M. Uhrig, Phys. Rev. Lett. **76** (1996) 208.
[8] N. Andersen and K. Bartschat, J. Phys. B **27** (1994) 3189; *corrigendum*: J. Phys. B **29** (1996) 1149.
[9] N. Andersen and K. Bartschat, *Polarization, Alignment, and Orientation in Atomic Collisions*, Springer-Verlag (New York, Heidelberg, 2001).
[10] N. Andersen, K. Bartschat, J. T. Broad, and I. V. Hertel, Phys. Rep. **279** (1997) 251.
[11] M. A. Khakoo and J. W. McConkey, J. Phys. B **20** (1987) 5541, and references therein.
[12] K. E. James, Jr., J. G. Childers. and M. A. Khakoo, Phys. Rev. A **69** (2004) 022710.
[13] http://physics.nist.gov/cgi-bin/ASD/lines1.pl
[14] W. B. Westerveld, K. Becker, P. W. Zetner, J. J. Corr, and J. W. McConkey, Appl. Opt. **24** (1985) 2256.
[15] Edmund Optics, 101 East Gloucester Pike, Barrington, NJ 08007, USA, model NT01-913-566.
[16] K. Palik, *Handbook of Optical Constants*, Academic (New York, 1985), p. 81.
[17] J. R. Samson, *Techniques of Ultraviolet Spectroscopy*, John Wiley & Sons (New York, 1967) Ch. 9.
[18] O. Zatsarinny and K. Bartschat, J. Phys. B. **37** (2004) 2173.
[19] O. Zatsarinny, Comp. Phys. Commun. **174** (2006) 273.
[20] http://ie.lbl.gov/education/parent/ne_iso.htm